PHYSICAL REVIEW E **71**, 015204(R) (2005)

Stability of flow- and diffusion-distributed structures to inlet noise effects

Pavel V. Kuptsov*
Centre for Mathematical Science, City University, Northampton Square, London EC1V 0HB, United Kingdom

Razvan A. Satnoianu†
Faculty of Actuarial Science, Cass Business School, City University, London EC1Y 8TZ, United Kingdom
(Received 26 July 2004; published 14 January 2005)

Stationary flow- and diffusion-distributed structures (FDS) patterns appear in a reaction-diffusion-advection system when a constant forcing is applied at the inlet of the reactor. We show that if the forcing is subject to noise, the FDS can be destroyed via the noise-induced Hopf instability. However, the FDS patterns are restored if the flow rate is sufficiently high. We demonstrate that the critical flow rate which is required for the stabilization of FDS has a power-law dependence on the noise amplitude.

DOI: 10.1103/PhysRevE.71.015204 PACS number(s): 82.40.Ck, 47.54.+r, 47.70.Fw, 82.20.−w

Flow- and diffusion-distributed structures (FDS) are a relatively new type of stationary pattern formed in reaction-diffusion systems in the presence of an open flow. These patterns appear due to a constant forcing being applied at the inlet boundary of the reactor when the flow rate becomes sufficiently high [1–5]. If the inlet is subjected to fluctuations, the FDS may be destroyed. This was reported in the experimental works [6,7]. The FDS was observed for sufficiently high flow rate while slowing down the flow results in the appearance of nonstationary structures.

The effect of the inlet noise on convectively unstable distributed systems was studied by a lot of authors. We recall that in a convectively unstable system the growing perturbation drifts with the flow and decays when observed from a fixed point. On the other hand, the absolute instability of the system means that the initially localized perturbation gives rise to a nonzero amplitude pattern at any fixed point in space [1,8–10] (see also therein references to the earlier works). Due to the extreme sensitivity of the convectively unstable state to perturbations, several authors [11–13] conclude that wave patterns may be generated and sustained due to amplification of fluctuations from an upstream noise source. A more subtle than a straightforward amplification of noise interplay between fluctuations and dynamics is revealed in [14] where the onset of turbulence in flow systems is treated as a kind of noise-induced transition. Kuznetsov [15] has studied the effect of the inlet noise on a spatially uniform reaction-diffusion-advection system. The noise-induced absolute instability is observed: the inlet noise increases the critical flow rate of transition from absolute to convective instability and the new critical value demonstrates the power-law dependence on the noise amplitude.

This paper describes the behavior of reaction-diffusion-advection systems that undergo a Hopf instability and also can sustain FDS patterns. We study the stability of the FDS when noise is applied at the inlet. Our concrete example is the well-known Lengyel-Epstein model for the chlorite-iodide-malonic acid-starch (CIMA) reaction [5,16,17],

$$u_t + \phi u_x - u_{xx} = a - u - 4uv/(1+u^2), \tag{1}$$

$$v_t + \phi v_x - \delta v_{xx} = b[u - uv/(1+u^2)]. \tag{2}$$

The chemical reactants are supplied at one end of the reactor and flow down through it at a speed ϕ. The dynamic variables $u(x,t)$ and $v(x,t)$ describe the concentrations of the two interacting chemical species, and δ is the ratio of the diffusion coefficients for these reagents. a and b stand for two other species presented in excess and are considered as kinetics parameters. This system allows for the uniform steady-state solution $u_S = a/5$ and $v_S = 1 + a^2/5^2$ which can lose its stability via either the Hopf or the Turing bifurcation. The critical points as obtained from the linear stability analysis are $b_H = (3a^2 - 5^3)/(5a)$, $b_T = \delta[5^3 + 13a^2 - 4a\sqrt{10(5^2+a^2)}]/(5a)$, respectively. Below we shall restrict ourselves to the case of the Hopf instability taking $b_H > b_T$ and $b < b_H$ (for the CIMA system supercritical values of b lie below bifurcation points). Although the Hopf bifurcation can be either super- or subcritical, our analysis remains valid in both cases since we consider the system far from the bifurcation point.

In the presence of constant inlet forcing a stationary structure appears near the inlet, which decays in space if the flow rate is small. When the flow rate grows, the uniform steady state u_S and v_S becomes spatially unstable with respect to perturbations that are constant in time [1,2]. Using this condition we obtain from the dispersion equation the critical point ϕ_{FDS} above which the constant inlet forcing gives rise to a nondecaying FDS [5],

$$\phi_{FDS} = \sqrt{\frac{40a^3b(\delta+1)^2 - (3a^2\delta + 5ab - 125\delta)^2}{(25+a^2)(\delta+1)(3a^2 - 5ab - 125)}}. \tag{3}$$

Note that the denominator vanishes at $b = b_H$, i.e., the domain of FDS coincides with the Hopf domain [4]. If the flow rate passes above ϕ_{FDS} while the Hopf instability is convective, i.e., $\phi > \phi_{FDS} > \phi_{ca}$, any small inlet perturbation grows to

*Corresponding author. Permanent address: Department of Informatics, Saratov State Law Academy, Chernyshevskaya 104, Saratov 410056, Russia. Electronic address: kupav@mail.ru
†Electronic address: r.a.satnoianu@city.ac.uk

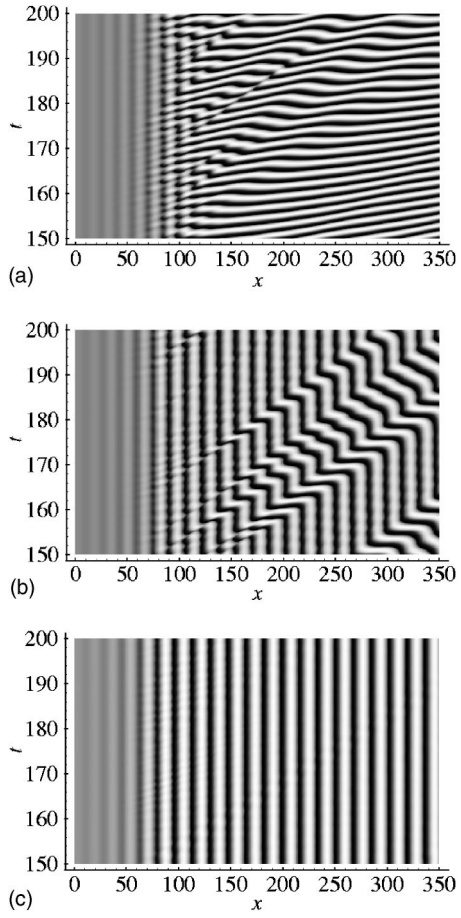

FIG. 1. FDS in the presence of the boundary noise. The flow rate grows from (a) $\phi=6$ to (b) $\phi=6.5$ and to (c) $\phi=7$. In panel (a) the noise destroys the FDS and induces the absolute Hopf instability, while in panel (c) FDS is stabilized by the high flow rate. $a=20$, $b=6$, $\delta=3$, $u_{\mathrm{bnd}}=0.1$, $\theta=0.05$.

FDS (here ϕ_{ca} is the critical point of the transition from absolute to convective instability that can be found from the dispersion equation of a system [8,9]). This case is referred to as a soft transition to FDS [10,18]. But if, however, $\phi_{\mathrm{ca}}>\phi>\phi_{\mathrm{FDS}}$, the expanding FDS appears provided that the flow rate and the inflow forcing are sufficiently high. This is the case of the rigid transition to FDS [10,18]. Below we shall concentrate on the case of the soft transition.

The inlet boundary condition in the presence of noise takes the form

$$u(x=0,t)=u_S+u_{\mathrm{bnd}}[1+\theta\xi(t)],\quad v(x=0,t)=v_S. \qquad (4)$$

Here u_S and v_S is the uniform steady state, u_{bnd} is the constant part of the inlet forcing, $\xi(t)\in[-1,1]$ is the noise with uniform distribution, and θ controls the noise amplitude. We also checked the response to Gaussian noise and obtained qualitatively similar results.

Figure 1 presents numerical solutions to the system (1) and (2). Here and below the solutions are obtained via a semi-implicit Cranck-Nicholson scheme with the steps of discretization $\Delta x\approx 0.1$ and $\Delta t\approx 0.0125$. The figure describes three typical cases observed in the presence of the inlet noise

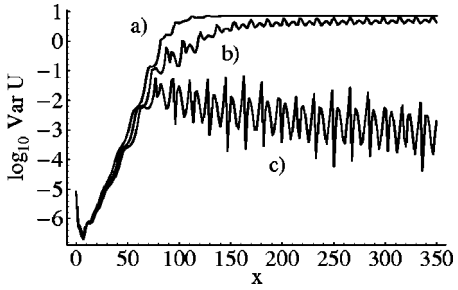

FIG. 2. Spatial distributions of the time variance for diagrams in Fig. 1 (the letters correspond to the panels of Fig. 1). Decaying of the curve (c) confirms the stabilization of the FDS at high flow rate as observed in Fig. 1(c).

(4) at different flow rates. The spatiotemporal diagrams in this figure are qualitatively similar to the experimental results in [6], Fig. 4 and in [7], Fig. 2(c).

In panel (a) of Fig. 1 the FDS appears near the inlet and grows until the temporal perturbations remain small. Then, around the point $x=75$ the FDS is destroyed. Behind this point the Hopf solution appears instead. Note the high regularity of this solution. The only source of the irregularity is the smooth variation in space of the phase of oscillations. This example is obtained for sufficiently small noise amplitude. Higher noise amplitude results in the higher irregularity to the phase distribution, but the whole structure remains ordered.

Panel (b) of Fig. 1 is obtained for a higher flow rate. As in the previous case, the FDS again grows from the inlet and the noise manifests itself at about $x=75$. From this figure one sees that the interval $0<x<75$ is nearly equal to the boundary layer where the FDS reaches its limiting amplitude. The influence of the noise in this panel is much weaker. The FDS pattern keeps its overall structure, but the stripes are cut and joined again with the shift between the upper and lower parts. This remarkable coordination between the FDS stripes and the wave of perturbation was earlier reported in the work of Kuptsov *et al.* [19], where the perturbation to FDS by the moving particle was studied. We also note that coexisting stationary and traveling waves have been observed in the system without noise [20].

In panel (c) of Fig. 1 the flow rate is increased even more. This results in the stabilization of FDS. Very small perturbations emerge near the point $x=75$ but rapidly decay, and the whole picture looks identical to the FDS without noise.

The curves in Fig. 2 present the spatial distributions of the variance calculated for the time series at every fixed point x for the solutions in Fig. 1. Obviously, the distribution is identically zero for ideal FDS. All the curves grow exponentially with nearly identical rates within the boundary layer of the FDS $0<x<75$. From this point the first curve (a), that correspond to the fully destroyed FDS in Fig. 1(a), rapidly slows down and reaches the saturated value at about $x=130$. The curve (b) drawn for the intermediate case in Fig. 1(b) behaves qualitatively similar as the previous one but its approaching to the limiting value is much slower. On the contrary, the curve (c) corresponding to the stable FDS in Fig. 1(c) decays exponentially behind the point $x\approx 75$. This clearly indicates that the FDS in Fig. 1(c) is indeed insensi-

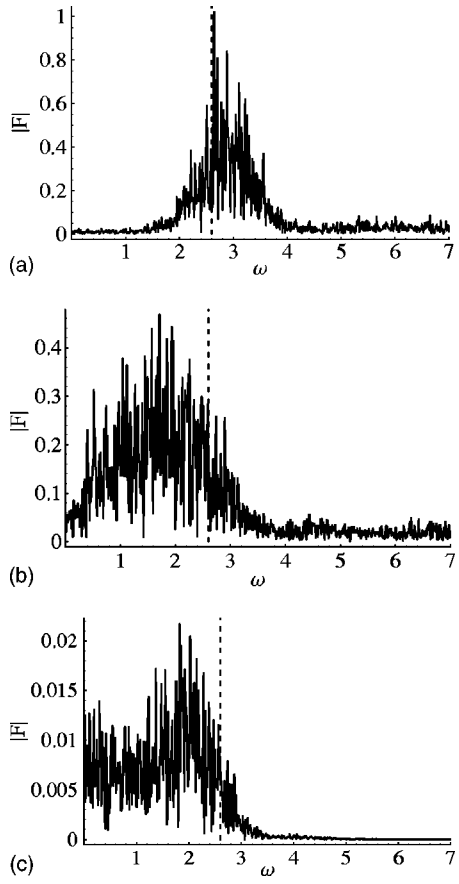

FIG. 3. Fourier spectra of time oscillations near the outlet for solutions in Fig. 1. The dashed lines indicate the Hopf frequency. Note that in panel (a) the Hopf frequency dominates, while in panels (b) and (c) frequency band shifts to the low-values area.

tive to the noise and it is not destroyed even far ahead from the inlet.

Above we have observed that when the FDS is destabilized by the noise, the Hopf solution appears behind. To provide a more careful verification of this observation, we present in Fig. 3 the Fourier spectra of the temporal oscillations near the outlet. Figure 3(a) corresponds to Fig. 1(a) and presents the case of the destabilization. Though the inlet noise has a uniform spectrum, the frequency selection takes place so that the spectrum at the outlet is sufficiently narrow. The bulk of spikes in the spectrum is located a little bit above the Hopf frequency indicated by the dashed line. This shift appears because the Hopf structure is not perfectly homogeneous in space. As seen from Fig. 1(a), deformations of the structure are distributed by the flow and appearing traveling waves result in increasing of the dominating frequency. So, we can conclude that the temporal oscillations in this case are mostly determined by the internal kinetics of the system. In the intermediate panel (b) low-frequency harmonics are mostly selected. The humplike structure of the spectrum corresponds to the horizontal bars that join shifted stripes in Fig. 1(b). Finally, for the case of the stabilization in panel (c) the spectrum becomes more uniform while the amplitudes of the spikes are very small.

Transition from panel (a) to panel (c) in Fig. 1 indicates

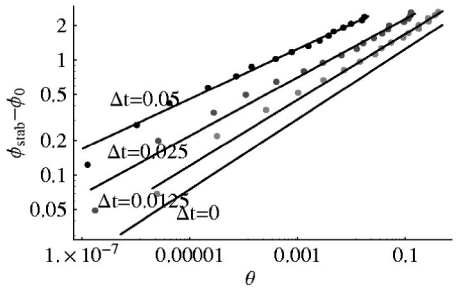

FIG. 4. Stabilization flow rate ϕ_{stab} vs the noise amplitude θ for different steps of the temporal numerical grid. $a=20$, $b=6$, $\delta=3$, $\phi_{FDS}=4.46$. Step of the spatial grid is $\Delta x=0.1$. Points present the numerical data and the lines are the approximating functions (5). Line $\Delta t=0$ is obtained via the extrapolation and have the coefficients $\phi_0=5.27$, $\chi=2.52$, and $\sigma=0.31$.

that there exists the critical flow rate ϕ_{stab} at which the stabilization of the FDS takes place. Let us find this critical value and analyze its dependence on the noise amplitude. First of all, we need to estimate the degree of FDS pattern destruction. For this purpose the variances of the temporal oscillations are calculated at fixed values of x within some interval near the outlet and then these variances are averaged. We have considered that the FDS is destroyed if the mean variance $\overline{\mathrm{Var}}$ is above the threshold 0.1 [this is the maximal value of the variance (c) in Fig. 2]. For given $\phi=\phi_{stab}$ the respective noise amplitude θ can be found as the numerical solution to the equation $\overline{\mathrm{Var}}(\theta)=0.1$. Performing this procedure for different ϕ_{stab} we obtain the dependence $\phi_{stab}(\theta)$. This function is found to be approximated well by the power law

$$\phi_{stab} = \phi_0 + \chi\theta^{\sigma}, \tag{5}$$

where ϕ_0, χ, and σ can be calculated from the numerical data by the least-squares method. This is shown in Fig. 4. We observe that increasing the noise intensity requires a higher stabilizing flow rate; vice versa, the growth of the flow rate makes the FDS less sensitive to the noise.

The data and the approximating coefficients depend on the step of the temporal discretization Δt that is applied to find the numerical solutions of Eqs. (1) and (2). (We found, however, that the data are insensitive to the spatial grid step Δx.) To estimate the function $\phi_{stab}(\theta)$ for the continuous system, we use linear extrapolation and find the coefficients $\phi_0(\Delta t)$, $\chi(\Delta t)$, and $\sigma(\Delta t)$ at $\Delta t=0$. The extrapolating graph is shown in Fig. 4.

The extrapolated ϕ_0, that is written in the caption of Fig. 4, is definitely higher than ϕ_{FDS}. It means that for the flow within the interval $\phi_{FDS}<\phi<\phi_0$ the FDS pattern is absolutely sensitive to the noise: the noise, regardless of its amplitude, always destroys the FDS. This, in particular, obstructs the experimental verification of the critical flow rate ϕ_{FDS}.

We have checked several parameter sets and observed that the width of the zone of the absolute sensitivity $\phi_0-\phi_{FDS}$ depends on the control parameters a and b but is varied sufficiently slowly with u_{bnd} and δ. The coefficients of the

approximating function σ and χ depend both on a and b and on u_{bnd} and δ.

The destruction and stabilization of the FDS in the presence of the noise can be treated as an implementation of a noise-induced absolute instability. In the noiseless system the Hopf mode is convectively unstable and the FDS expands over the whole space. If the noise is applied at the inlet, the FDS pattern performs a kind of a frequency selection that is controlled by the flow rate. When the flow rate is sufficiently small, the selected frequencies are resonant to the Hopf frequency. As a result, the noise-induced absolute Hopf instability takes place. When the flow rate is above the critical point, the selected frequencies are detuned from the resonance. The absolutely unstable Hopf mode is not excited and the FDS pattern becomes stable. The Hopf mode in this case is convectively unstable again.

The critical flow rate demonstrates the power-law dependence on the noise amplitude. Similar dependence is reported by Kuznetsov [15] for the system with the uniform boundary perturbed by the noise. Thus, we can conclude that this is one of the characteristic features of the noise-induced absolute instability.

We have studied the particular case of the FDS which forms when the Hopf oscillatory solution is allowed in the system, and it is this solution that appears when the noise destructs the FDS. On the other hand, the FDS is known to appear when the Hopf mode is stable [4,5]. It is interesting to analyze the stability of the FDS in this case. This will be the subject of our subsequent paper.

P.V.K. acknowledges support from the Royal Society and NATO/British FCO Chevening Postdoctoral Fellowship Programme.

[1] S. P. Kuznetsov, E. Mosekilde, G. Dewel, and P. Borckmans, J. Chem. Phys. **106**, 7609 (1997).
[2] P. Andresén, M. Bache, E. Mosekilde, G. Dewel, and P. Borckmans, Phys. Rev. E **60**, 297 (1999).
[3] M. Kærn and M. Menzinger, Phys. Rev. E **60**, R3471 (1999).
[4] R. A. Satnoianu and M. Menzinger, Phys. Rev. E **62**, 113 (2000).
[5] R. A. Satnoianu, P. K. Maini, and M. Menzinger, Physica D **160**, 79 (2001).
[6] M. Kærn and M. Menzinger, J. Phys. Chem. A **106**, 4897 (2002).
[7] A. F. Taylor, J. R. Bamforth, and P. Bardsley, Phys. Chem. Chem. Phys. **4**, 5640 (2002).
[8] W. van Saarloos, Phys. Rev. A **37**, 211 (1988).
[9] W. van Saarloos, Phys. Rev. A **39**, 6367 (1989).
[10] P. V. Kuptsov, S. P. Kuznetsov, C. Knudsen, and E. Mosekilde, in *Recent Research Development in Chemical Physics*, Vol. 4 (Transworld Research, Kerala, India, 2003), pp. 633–658.
[11] R. J. Deissler, J. Stat. Phys. **40**, 371 (1985).
[12] R. J. Deissler and J. D. Farmer, Physica D **55**, 155 (1992).
[13] P. Borckmans, G. Dewel, A. D. Witt, and D. Walgraef, in *Chemical Waves and Patterns*, edited by K. S. R. Kapral (Kluwer, Dordrecht, 1995).
[14] P. S. Landa, Europhys. Lett. **36**, 401 (1996).
[15] S. P. Kuznetsov, Math. Comput. Simul. **58**, 435 (2002).
[16] I. Lengyel and I. R. Epstein, Science **251**, 650 (1991).
[17] I. Lengyel and I. R. Epstein, Proc. Natl. Acad. Sci. U.S.A. **89**, 3866 (1992).
[18] P. V. Kuptsov, Physica D **197**, 174 (2004).
[19] P. V. Kuptsov, S. P. Kuznetsov, and E. Mosekilde, Physica D **163**, 80 (2002).
[20] R. A. Satnoianu, Phys. Rev. E **68**, 032101 (2003).